Journal of the Taiwan Institute of Chemical Engineers

Interaction of fusion temperature on the magnetic free convection of nano-encapsulated phage change materials within two rectangular fins-equipped porous enclosure

--Manuscript Draft--

Manuscript Number:	
Article Type:	SI:Nano-Renewable
Section/Category:	Energy and Environmental Science and Technology
Keywords:	NEPCMs; Fins-equipped porous enclosure; Rayleigh number; FEM; Magnetic field
Corresponding Author:	A.S. Dogonchi Aliabad Katoul, IRAN (ISLAMIC REPUBLIC OF)
First Author:	A.S. Dogonchi
Order of Authors:	A.S. Dogonchi
	S.R. Mishra
	Nader Karimi
Abstract:	The present study encountered the impact of non-dimensional fusion temperature on the free convection of conducting nanofluid within a porous enclosure filled with nano-encapsulated phage change materials (NEPCMs). The enclosure is equipped with two parallel fins that have ability to move in both the directions such as vertically as well as horizontally. In particular the particles are structured as core-shell with phase change materials. The enclosure is designed in such a way that both the top and bottom walls are insulated whereas the isothermal vertical walls are heated differentially. The phage change of the materials is obtained fro the solid to liquid and absorbs the surrounding temperature in the hot region and released in the cold region. The governing transformed equations are tackled by using robust Finite Element Method. The numerical simulation of the isotherms, streamlines and heat transfer coefficient ratio along with velocity distribution for various parameters are presented. These are affecting a key role on the average and local Nusselt number as well as on the local Bejan number. However, the measure outcomes are; both the longitudinal and transverse velocity profiles boosts up with an augmented Rayleigh number however, the weaker flow field is generated for the increasing Hartmann number.
Suggested Reviewers:	Khalil Ur Rehman, PhD University of Waterloo kurrehman@uwaterloo.ca
	Abdelraheem M. Aly, PhD King Khalid University ababdallah@kku.edu.sa
	W.A. Khan, PhD Beijing Institute of Technology waqarazeem@bit.edu.cn
	Muhammad Waqas, PhD National University of Technology muhammadwaqas@nutech.edu.pk
	Taher Armaghani, PhD Islamic Azad University armaghani.taher@yahoo.com
	S.M. Seyyedi, PhD Islamic Azad University s.masoud_seyedi@aliabadiau.ac.ir
	M. Nawaz, PhD

	nawaz_d2006@yahoo.com
Opposed Reviewers:	

COVER LETTER FOR SUBMISSION OF MANUSCRIPT

Subject: **Submission of manuscripts**

Dear Editor,

With this letter, I have attached a copy of manuscript entitled "**Interaction of fusion temperature on the magnetic free convection of nano-encapsulated phage change materials within two rectangular fins-equipped porous enclosure**". It is declared that the work described has not been published previously, that it is not under consideration for publication elsewhere, that its publication is approved by all authors and that, if accepted, it will not be published elsewhere in the same form, in English or in any other language, without the written consent of the Publisher.

With best wishes and highest personal regards.

Sincerely yours,

A.S. Dogonchi

Please check the following points before submitting the pdf file for your manuscript. Manuscripts that do not conform may be returned for correction and resubmission. You should be able to answer "yes" to all of the following questions.

- Is the manuscript double-spaced with a font size of 12 pt (Times or Times New Roman preferred)?

  YES

- Have you given full addresses and affiliations for all co-authors?

  YES

- Is the corresponding author identified by an asterisk (*) and their contact details (phone number and e-mail address) given on the first page?

  YES

- Have you given a Graphical Abstract and Highlights of your manuscript?

  YES

- Does the manuscript include a one-paragraph abstract of no more than 200 words for Original Papers or 150 words for Short Communications?

  YES

- Do the length of manuscript and the number of display items obey the requirement?

  YES

- Have keywords (maximum 6) been provided immediately after the abstract?

  YES

- Are sections given Arabic numbers with subsections numbered using the decimal system? NOTE: Acknowledgements and References sections are **not** numbered.

  YES

- Do you embed all figures, tables, and schemes (including the captions) at appropriate places in the text?

  YES

- Are References in the correct format for this journal?

  YES

- Are all references mentioned in the Reference list cited in the text, and vice versa?

YES

- Has the manuscript been spell-checked and grammar-checked?

  YES

- Are all symbols translated correctly in the pdf file?

  YES

- Has written permission been obtained and uploaded as Additional Files for use of copyrighted materials from other sources (including illustrations, tables, text quotations, Web content, etc.)? Has the copyright information been included in the relevant figure caption or table footnote, as an example "Reprinted with permission from Ref. [10]. Copyright 2010 Elsevier"?

  YES

Research Highlights:

- Entropy generation and hydrothermal analyses in a NEPCMs-filled enclosure are done.
- The fins-equipped porous enclosure is subject to a magnetic field.
- The fins have the potential to move vertically and horizontally.
- The FEM is utilized to solve the governing equations.
- Altering the characteristics of the fins could play a vital role.

Interaction of fusion temperature on the magnetic free convection of nano-encapsulated phage change materials within two rectangular fins-equipped porous enclosure

A. Sattar Dogonchi[1*], S.R. Mishra[2], Nader Karimi[3]

[1]Independent researcher in Mechanical Engineering
[2]Siksha 'O' Anusandhan University, Bhubaneswar, Odisha 751030, India,
[3]School of Engineering and Materials Science, Queen Mary University of London, London, United Kingdom,
***Corresponding author(s):** A. Sattar Dogonchi
(Email address: a.s.dogonchi@gmail.com, phone number: +98112707743)

Abstract:

The present study encountered the impact of non-dimensional fusion temperature on the free convection of conducting nanofluid within a porous enclosure filled with nano-encapsulated phage change materials (NEPCMs). The enclosure is equipped with two parallel fins that have ability to move in both directions such as vertically as well as horizontally. In particular the particles are structured as core-shell with phase change materials. The enclosure is designed in such a way that both the top and bottom walls are insulated whereas the isothermal vertical walls are heated differentially. The phage change of the materials is obtained fro the solid to liquid and absorbs the surrounding temperature in the hot region and released in the cold region. The governing transformed equations are tackled by using Finite Element Method. The numerical simulation of the isotherms, streamlines and heat transfer coefficient ratio along with velocity distribution for various parameters are presented. These are affecting a key role on the average and local Nusselt number as well as on the local Bejan number. However, the measure outcomes are; both the longitudinal and transverse velocity profiles boosts up with an augmented Rayleigh number however, the weaker flow field is generated for the increasing Hartmann number.

Keywords: NEPCMs; Fins-equipped porous enclosure; Rayleigh number; FEM; Magnetic field.

1. Introduction

In recent era of science and technology depends upon the use of nanofluids because of its greater heat transfer performances. The enhanced performances are due to the raised thermophysical properties and conceivable thermal energy transfer fluids that can be activated in various electronic devices for better enforcement. Depending upon various resources and transport, the size of the particle affects and play a significant role in the study of nanotechnology. In different field of research i.e. operations in medical, electrical fields, etc. there is an extensive application of nanoparticles. In these areas the considered particles are allowed only depending upon their diameter. Flow of fluid between two parallel walls, channels, cavity, etc. has attracted various researchers to develop the mechanics and to enhance the thermal properties. In connection to the potential applications in engineering, as well as industries the study on these phenomena creates enormous interest to young scientists. The metal purifications in fluid, food stuff, compression and injection shaping, etc. coined as soe engineering application and chemical industries, biochemical technology, petroleum, and manufacture of medicine [1–5] are several industrial applications where the use of nanofluid is extensive. Ibrahim and Terbeche [6] and Watanabe and Pop [7] proposed their discussion on the behaviour of the magnetic field for the flow of conducting nanofluid past a flat wall. However, Khaled and Vafai [8] have analyzed the impact of magnetic strength for the oscillatory thin films and in their study they have disclose the behaviour showing properties of magnetic strength that decrease the flow change abilities inside thin films. The issue is raised due to the squeezing flow analysis. However, the aforesaid studies have some lacking in various phenomena on the thermal and diffusion transfer that will past through the walls with sensor located within the fluidic cells. These studies are accountable to squeezing flow analysis. In comparison to solid nanoparticles, the traditional fluids such as water, kerosene (oil), ethylene glycol, etc. have weak conductivity. Therefore, to enrich the thermal conductivity, the solid nanoparticles are suspended into the base (conventional) fluids. The integration of these nanoparticles of both metal and oxides within the base fluid that provides the superior heat transfer rate.

As a new approach the consideration of Nano-Encapsulated Phase Change Materials (NEPCMs) can be used for the preparation of nanofluids. Here, these nanoparticles are consists of a core and a shell. Moreover, Phase Change Material (PCM) is used for the preparation of the core part. In a particular fusion temperature, solid-liquid phase change is obtained by PCM and significant aount of energy is released/absorbed because of latent heat of the phase change [9]. In recent studies Fang et al. [10] proposed a nanofluid using NEPCM suspensions in which for the core they have employed n-tetradecane and for the polymer shell they have used formaldehyde. Further, Qiu et al. [11] considered n-octadecane for the core and for the shell they have proposed methylmethacrylate (MMA)-based polymer to prepare a nanofluid using NEPCM nanoparticles. Recently, admirable reviews on the PCMs either nano/ micro capsulation for the heat transport performances has been carried out by various researchers such as Jamekhorshid et al. [12] and Su et al. [9]. In particular for the storage of the thermal energy the application of PCMs play a vital role. The extensive studies in this regards is proposed by Pielichowska and Pielichowski [13]. For the building of thermal management again there is an extensive applications for the use of PCMs. Keshteli and Sheikholeslami [14] carried out the intensification of the theral performances building and Huang et al. [15] proposed the Morphological characterization of the PCMs. However, Moreno et al. [16] used several phase change aterials for the domestic applications such as heat pump and air-conditioning systems.

Various studies have been designed for the simulation of free convection on the nanofluid flow of various materials within enclosures. The theral enhancement for the flow phenomena of various nanofluids within a wavy wall cavity has been proposed by Hashim et al. [17] and Asabery [18]. Further, Sivaraj and Sheremet [19] investigated their studies on the free convection of nanofluids enclosed by a cavity where both the plates are heated. An analysis is carried out for the flow properties of nanofluid past through a preamble ediu by various researchers like Ghalambaz et al. [20] and Tahmasebi et al. [21].

2. Governing Equations

Magnetic natural convection taken place within a novel porous enclosure filled with NEPCMs and equipped with two rectangular fins which possess the ability to move vertically and horizontally is scrutinized. The governing equations for such a system may well be demonstrated as:

$$\frac{\partial u}{\partial x}+\frac{\partial v}{\partial y}=0 \tag{1}$$

$$\rho_b\left(u\frac{\partial u}{\partial x}+v\frac{\partial u}{\partial y}\right)=-\frac{\partial p}{\partial x}+\mu_b\left(\frac{\partial^2 u}{\partial x^2}+\frac{\partial^2 u}{\partial y^2}\right)+B_0^2\delta_b\begin{pmatrix}\cos(\gamma)\sin(\gamma)v\\-\sin(\gamma)\sin(\gamma)u\end{pmatrix}-\frac{\mu_b}{K}u \tag{2}$$

$$\rho_b\left(u\frac{\partial v}{\partial x}+v\frac{\partial v}{\partial y}\right)=-\frac{\partial p}{\partial y}+\mu_b\left(\frac{\partial^2 v}{\partial x^2}+\frac{\partial^2 v}{\partial y^2}\right)+B_0^2\delta_b\begin{pmatrix}\cos(\gamma)\sin(\gamma)u\\-\cos(\gamma)\cos(\gamma)v\end{pmatrix}-\frac{\mu_b}{K}v+\rho_b\beta_b g\left(T-T_c\right) \tag{3}$$

$$\left(\rho C_p\right)_b\left(u\frac{\partial T}{\partial x}+v\frac{\partial T}{\partial y}\right)=k_b\left(\frac{\partial^2 T}{\partial x^2}+\frac{\partial^2 T}{\partial y^2}\right) \tag{4}$$

ρ_b, $(\rho Cp)_b$, β_b, μ_b, δ_b and k_b are defined as follows:

$$\rho_b=(1-\phi)\rho_f+\phi\rho_p,\ \beta_b=(1-\phi)\beta_f+\phi\beta_p,\ \left(\rho C_p\right)_b=(1-\phi)\left(\rho C_p\right)_f+\phi\left(\rho C_p\right)_p \tag{5}$$

$$\mu_b=\mu_f\left(1+N_v\phi\right),\ \delta_b=\delta_f\left(1+N_e\phi\right),\ k_b=k_f\left(1+N_c\phi\right) \tag{6}$$

where N_v, N_e, and N_c signify the numbers of dynamic viscosity, electrical conductivity, and thermal conductivity, respectively. The governing equations must be converted to their non-dimensional type, the following expressions, therefore, should be characterized:

$$X=\frac{x}{L},\quad Y=\frac{y}{L},\quad P=\frac{pL^2}{\rho_f\alpha_f^2},\quad U=\frac{uL}{\alpha_f},\quad V=\frac{vL}{\alpha_f},\quad \theta=\frac{T-T_c}{T_h-T_c} \tag{7}$$

so the dimensionless type of governing equations could be derived as:

$$\left(U\frac{\partial U}{\partial X}+V\frac{\partial U}{\partial Y}\right)=-\frac{1}{\rho_b/\rho_f}\frac{\partial P}{\partial X}+\frac{(1+N_v\phi)}{\rho_b/\rho_f}\Pr\left(\frac{\partial^2 U}{\partial X^2}+\frac{\partial^2 U}{\partial Y^2}\right)+\frac{(1+N_e\phi)}{\rho_b/\rho_f}Ha^2\Pr\begin{pmatrix}\cos(\gamma)\sin(\gamma)V\\-\sin(\gamma)\sin(\gamma)U\end{pmatrix}-\frac{(1+N_v\phi)}{\rho_b/\rho_f}\frac{\Pr}{Da}U \tag{8}$$

$$\left(U\frac{\partial V}{\partial X}+V\frac{\partial V}{\partial Y}\right)=-\frac{1}{\rho_b/\rho_f}\frac{\partial P}{\partial Y}+\frac{(1+N_v\phi)}{\rho_b/\rho_f}\Pr\left(\frac{\partial^2 V}{\partial X^2}+\frac{\partial^2 V}{\partial Y^2}\right)+\frac{(1+N_e\phi)}{\rho_b/\rho_f}Ha^2\Pr\begin{pmatrix}\cos(\gamma)\sin(\gamma)U\\-\cos(\gamma)\cos(\gamma)V\end{pmatrix}-\frac{(1+N_v\phi)}{\rho_b/\rho_f}\frac{\Pr}{Da}V+\frac{\beta_b}{\beta_f}\Pr Ra\theta \tag{9}$$

$$C_r\left(U\frac{\partial \theta}{\partial X}+V\frac{\partial \theta}{\partial Y}\right)=(1+N_c\phi)\left(\frac{\partial^2 \theta}{\partial X^2}+\frac{\partial^2 \theta}{\partial Y^2}\right) \tag{10}$$

Subject to the boundary conditions:

$$\begin{aligned}&\theta=1 && \text{on the fins as well as hot wall}\\&\theta=0 && \text{on the cold wall}\\&\partial\theta/\partial n=0 && \text{on the other wall}\\&\Psi=0 && \text{on all walls}\end{aligned} \tag{11}$$

here C_r (heat capacity ratio) could be defined as:

$$C_r=\frac{(\rho C_p)_b}{(\rho C_p)_f}=(1-\phi)+\phi\lambda+\frac{\phi}{\chi Ste}f \tag{12}$$

in equation (12), f and Ste signify the dimensionless fusion function and the Stefan number, respectively. The former could be determined as [22]:

$$f=\frac{\pi}{2}\sin\left(\frac{\pi}{\chi}\left(\theta-\theta_f+\frac{\chi}{2}\right)\right)\times\begin{cases}0 & \theta<\theta_f-\frac{\chi}{2}\\1 & \theta_f-\frac{\chi}{2}<\theta<\theta_f+\frac{\chi}{2}\\0 & \theta>\theta_f+\frac{\chi}{2}\end{cases} \tag{13}$$

here θ_f indicates dimensionless fusion temperature.

The Local and average Nusselt numbers along the cold wall can be defined as:

$$Nu_{loc.} = -\frac{k_b}{k_f}\frac{\partial \theta}{\partial n}\ ,\ Nu_{ave.} = \frac{1}{S}\int_0^S Nu_{loc.} ds \qquad (14)$$

3. Entropy generation

According to [23], the local and total entropy generation (En_{local}, En_{total}) for the above-mentioned problem could be demonstrated as:

$$En_{local} = \underbrace{(1+N_c\phi)\left[\left(\frac{\partial\theta}{\partial Y}\right)^2 + \left(\frac{\partial\theta}{\partial X}\right)^2\right]}_{En_{local,HT}} + \underbrace{(1+N_v\phi)\,\varepsilon_f\left[\begin{array}{c} 2\left(\frac{\partial U}{\partial Y}\right)^2 + 2\left(\frac{\partial U}{\partial X}\right)^2 \\ +\left(\frac{\partial U}{\partial X} + \frac{\partial U}{\partial Y}\right)^2 \end{array}\right]}_{En_{local,FF}} \qquad (15)$$
$$+\underbrace{(1+N_e\phi)\,\varepsilon_f\,Ha^2\left(U\sin(\gamma) - V\cos(\gamma)\right)^2}_{En_{local,MF}} + \underbrace{(1+N_v\phi)\frac{\varepsilon_f}{Da}\left(U^2+V^2\right)}_{En_{local,PM}}$$

$$En_{total} = \int_V En_{local}\,\mathrm{dV}. \qquad (16)$$

Based on the definition of the En_{local} and En_{total}, we could easily define the Bejan number (Be_{local}, Be_{ave}) as:

$$Be_{local} = En_{local,HT} / En_{local}$$
$$Be_{ave.} = \int_A Be_{local}\,\mathrm{dA} \Big/ \int_A \mathrm{dA} \qquad (17)$$

4. Numerical solution and validation

The present research work demonstrates the natural convection of nanofluid equipped with NEPCMs. The fluid past within a novel porous enclosure equipped with two rectangular fins that possess the ability to move the liquid both vertically and horizontally (**Fig.1**). The inclusion of inclined magnetic field is also scrutinized to show the credibility of the magnetism on the free convective fluid. The transformed coupled equations (8-10) comprised of both the flow and heat transfer phenomenon along with the appropriate boundary conditions (11) are handled by finite element method. The weak forms of the governing equations are presented and discritized over a non-uniform structure grid. Then mathematical software is used to simulate the results. The iteration process is continued till to get a desire accuracy of 10^{-5}. The details of the procedure are explained in [24]. The validation of the present code with other numerical results of Khanafer et al. [25] and experimental work of Krane and Jessee [26] is obtained and exhibited in **Fig.2**. Based on this figure, we could undoubtedly trust our results.

5. Results and discussion

The impact of diverse parameters like Rayleigh number (*Ra*), dimensionless fusion temperature (θ_f), the Stefan number (Ste), Hartmann number (Ha), Inclination angle of magnetic field (γ), δ, Darcy number (Da) and *AR* on magnetic natural convection taken place within a porous enclosure filled with NEPCMs and equipped with two rectangular fins. **Table-1** displays the variation of Rayleigh number, and Hartmann number for several values of nanoparticle volume fraction on the average Nusselt number. The numerical simulated results are presented for $Ra=10^4$ and $Ra=10^5$ by neglecting the interaction of magnetic field (Hartmann number, *Ha*=0) as well as inclusion of magnetic field (Hartmann number, *Ha*=40). Here, the nanoparticle volume fraction is considered within the range of 1% to 5%. It is seen that the boosts in the average Nusselt number is rendered for the augmentation in the nanoparticle volume fraction and the greater in the strength of Hartmann number. The trend of the profiles is due to the resistance of the body force caused by the inclusion of magnetic strength augment the heat transfer rate near the cold region. Moreover, increasing Rayleigh number also enriches the profile of average Nusselt number. Further, with some fixed values of certain parameters described earlier, the behaviour of characterizing parameters on the streamlines, isotherms and heat capacity ratio is presented. Also, the velocity distributions and local Nusselt number profiles are exhibited for various values of these parameters. Demonstration is carried out for the numerical results of $\left|\Psi_{\max}\right|_{nf}$, of the various flow pattern within the fins. The NEPCM particle is suspended in the base fluid to perform a dilute suspension and the volume fraction of the particle is considered to be within the range $0 \le \phi \le 0.05$. Considering the core-shell weight ration as nearly 0.7, n-octadecane as PCM with water as the base fluid and NEPCM filled within the porous shells the Stefan number is adopted as 0.313 and the heat capacity ratio is posted as 0.4. Within the range of the cold wall temperature to the hot wall temperature, the fusion temperature θ_f is considered as $0 < \theta_f < 1$. The number dynamics viscosity, N_v, as well as the thermal conductivity, N_c, are taken to be within the range 0<N_v, N_c <6. In the case of nanofluid, it is not desirable to neglect these values however, for various naoparticles these values can be considered greater than the proposed value. The larger values of N_v, and N_c indicates the larger viscosity and thermal conductivity. The core PCM is very much lighter than the water whereas the porous material is heavier to it. Therefore the density ratio between the particle and the base fluid is quantitatively less than unity. **Fig.3** demonstrates the behaviour of *Ra* and *Ha* on the isotherms, streamlines and the heat capacity ratio profiles. From the geometry of the proposed model it is seen that, both the fins are placed equidistance from the porous enclosures that deliberates the symmetrical nature of the profiles. Within the enclosures it is seen that, the velocity gradient upsurges that resulted in higher fluid density difference. This situation occurs due to an increase in *Ra*. However, irrespective of the presence (*Ha*=20, 40)/ the absence (*Ha* = 0), the flow field of nanofluid increases. For *Ha* =0, the variation of $\left|\Psi_{\max}\right|_{nf}$ is presented with its increasing behaviour as 0.133385 to 9.18653 (for *Ha* = 0), from $\left|\Psi_{\max}\right| = 0.079264$ to $\left|\Psi_{\max}\right| = 6.02857$ (for *Ha* =20) and $\left|\Psi_{\max}\right| = 0.079264$ to $\left|\Psi_{\max}\right| = 0.079264$ (For *Ha* =40). The range of Rayleigh number is $10^3 < Ra < 10^5$. Further, the weaker flow field is generated for the increasing Hartmann number. The fact is straight forward i.e. the inclusion of magnetic field causes an opposing force due to the production of Lorentz force. Heat transfer convection plays a vital role and is more significant. It is clear to observe that the bottom part of the fin layer become thinner and thinner due to the cold wall and consequently a plume starts at the upper part of the fin resulted in the isotherms moves upward. **Fig.4** portrays the influence of *Ra* and *Ha* on the longitudinal as well as the transverse velocity distribution for the 5% nanoparticle volume fraction. In the permeable region, for $Ha = 0$ and increasing *Ra* it is seen that both the velocity profiles *U* and *V* enhance in their corresponding directions. However, augmentation in the Hartmann number, the profiles retards significantly irrespective of the values of the Rayleigh number. Combined impact of both the resistive forces i.e. inclusion of magnetic field and porosity resists the velocity profiles. In fact, separation occurs due to the distinct vertical layers near the hot and cold walls of the fins. **Fig.5** deliberates the profiles of isotherms and the streamlines for the variation of *Da* and the Rayleigh number. As similar to the Hartmann number, due the inclusion of resistive force, porosity is also a resistive force that causes a similar trend on the isotherms and streamlines as described in **Fig.3**. Due the heavier nanoparticle density, the clogging of the particles is appeared near the lower region of the fin for both the cold and the hot wall. Therefore, the isotherms move closer towards the wall region. The flow field enlarges as $10^3 \le Ra \le 10^5$ within the range $0.133385 \le \left|\Psi_{\max}\right|_{nf} \le 9.18653$ in the permeable region. But for $Ra = 10^3$, with increasing permeability slower down the profiles and the flow rate decelerates from. $0.133385 \le \left|\Psi_{\max}\right|_{nf} \le 0.0217234$. Illustration of the velocity profiles for the variation of Porosity, *Da* versus *Ra* is presented in **Fig.6**. The observation is carried out for the 5% nanoparticle concentration and the presence of Hartmann number. An increase in Rayleigh number encountered a greater increasing rate in both the longitudinal and transverse velocity. It is seen that, movement of the fluid particle from the bottom of the colder fin region to hotter wall of the fin in a horizontal direction whereas the transverse profile also boots up in the vertical direction. The resistivity offered by the Porosity retards both the profiles significantly. The range of the longitudinal velocity for *Da* = 10^{-1} with the variation of *Ra* is $0.836193 \le |U_{\max}| \le 61.3767$ and the transverse velocity varies within the range $0.616095 \le |V_{\max}| \le 68.5884$. Moreover, for *Ra* =$10^3$ and the variation of *Da* from 10^{-1} to 10^{-3} the longitudinal velocity varies within the range $0.836193 \ge |U_{\max}| \ge 0.173736$ and transverse velocity varies as $0.616095 \ge |V_{\max}| \ge 0.16916$. **Fig.7** exhibits the distribution of isotherms, streamlines and the heat capacity ratio for the variation of phase angle, γ where $0^0 \le \gamma \le 90^0$. It is observed that, augmentation in the phase angle the velocity gradient decelerates irrespective of the values of Rayleigh number. However, the variation of phase angle on the velocity profiles shows its opposite impact as displayed in **Fig.8**. With an increasing γ within $0^0 \le \gamma \le 30^0$ the longitudinal velocity increases and further, within the range of $60^0 \le \gamma \le 90^0$ it decreases and in case of transverse velocity it is seen that the profile enhances within the range $0^0 \le \gamma \le 60^0$ and afterwards it lower down. **Fig.9** and **Fig.10** reveals the variation of isotherms, streamlines, heat capacity as well as the velocity distribution for the variation of fusion temperature respectively. The result shows its fluctuating nature for several values of fusion temperature on the profiles. The investigations of the enclosure's dimensional ratio (*AR*) and *Ra* on the profiles of isotherms, streamlines for the standard values of the contributing parameters i.e. $\phi = 5\%$, *Da*=0.01 and *Ha*=40 is displayed in **Fig.11** whereas the velocity distribution is presented in **Fig.12**. The rising *AR* enriches the flow field of nanofluid. As $10^3 \le Ra \le 10^5$ the flow field increases within the range $0.127198 \le |\Psi_{\max}| \le 11.9587$. Further, the longitudinal velocity enhances within the range $0.795556 \le |U_{\max}| \le 65.3443$. Irrespective the values of *Ra*, the gradient enhances significantly along with the velocity profiles. It can be seen, isotherm lines get closer to warm wall with increasing the dimensional ratio. The fact is fluid flow decreasing between the cold and warm walls. Raise in heat transfer is one of the factors for this observation. From the **Fig.13 and 14** the similar tendency is marked for the variation of the parameter δ. The entropy generation due to the irreversibility of the system is observed. Entropy is the measure of the thermal energy of the system per unit temperature that is not available for the construction of the work. The molecular disorder is also measured by the entropy analysis. However, the Bejan number is the pressure drop within the enclosure. The simulation of local Bejan number for various values of Rayleigh number within the certain range of Hartmann number and the porous matrix is displayed in **Fig.15**. From the figure it is seen that the local Bejan number decreases with increasing Rayleigh number also increasing Hartmann number and porosity with higher Rayleigh number the behaviour of the local Bejan number is insignificant. The that is the local Nusselt number is exhibited in **Fig.16**. The behaviour of different characterizing parameters i.e. *Ha*, *Ra*, and *AR* with augmented values of increasing the length of the hot wall is simulated and displayed. The activities of the profiles seem to be wavy due to assumed wavy boundary. It is clarified from the figure that, with increasing *Ra* the rate of heat transfer enhances further, the impact is opposite for the increasing *Ha*. It is interesting to note that with an increase of the length of the hot wall the local Nusselt number decreases. The heat transfer rate i.e. the local Nusselt number for the effects of AR, *Ra* and *Da* versus *Ha*, is displayed in **Fig.17**. The heat transfer rate enhances for the absence of porous matrix i.e. *Da*=100 in other words it retards in the presence of porous matrix i.e. *Da*=0.01. Moreover, the effects of *Ha* and *Ra* are similar as described earlier. **Fig.18** portrays the characteristics of average Nusselt number (Nu_{avg}) with the variation of δ, *Ra*, and *AR* versus *Ha*. As the range or *Ra* increases from 10^4 to 10^5 the retardation rate of Nu_{avg} is greater. In comparison to *Ha* it is seen that presence of *Ha* retards the coefficient significantly. Moreover, owing the growing values of *AR* significant decrease in Nu_{avg} is marked. Fig.19

portrays the behaviour of *Da* on the average Bejan number for the various values of Hartmann number i.e. *Ha*=0 and *Ha* = 40. It is observed that, increasing *Da* retards the average Bejan value irrespective of the values of Hartmann number.

6. Conclusive remarks

Free convection of nanofluid comprised of NEPCM nanoparticles suspended in the base fluid is investigated in the present study within a porous enclosure. Two parallel fins are placed horizontally where both the top and bottom walls are insulated. The release of latent heat and the absorption of NEPCM particle are obtained due to the phase change. Numerical scheme pertaining to Finite Element Method is used to tackle the transformed governing equations and simulation is carried out for the contributing parameter. In a novel approach the entropy generation due to the irreversibility process of the system is obtained and the computational results of local and average Bejan number are displayed via figures. However, the conclusive remarks for the measure outcomes are deliberated as;

- The validation of the current result with the earlier experimental result as well as the numerical results show a greater concurrency that gives a gate way to proceed the present work for the further investigation for various contributing parameters using the numerical scheme FEM.
- The contribution of NEPCM enriches the heat transfer criterion due to improving thermal conductivity and heat capacity for the fusion temperature of the particles.
- Augmentation in the nanoparticle volume fraction boosts up the average Nusselt number and the fact is due to the greater in the strength of Hartmann number. The heat transfer rate near the cold region enhances the profile to move towards the hot region. Moreover, growing Rayleigh number also enriches the profile of average Nusselt number.

- The velocity gradient retards for the increasing phase angle further decelerates both the longitudinal and transverse velocity distribution irrespective the variation of the Rayleigh number.
- Increasing *Ra* within its range, the average Nusselt number falls down significantly further, the presence of Hartmann number and enhancement in *AR* also decelerates the profile of Nu_{avg} significantly.

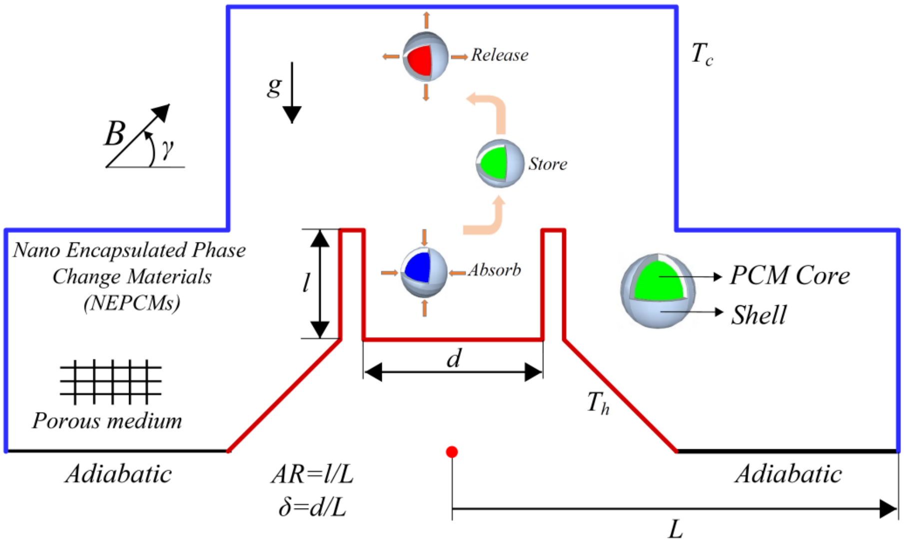

Fig. 1. The studied geometry

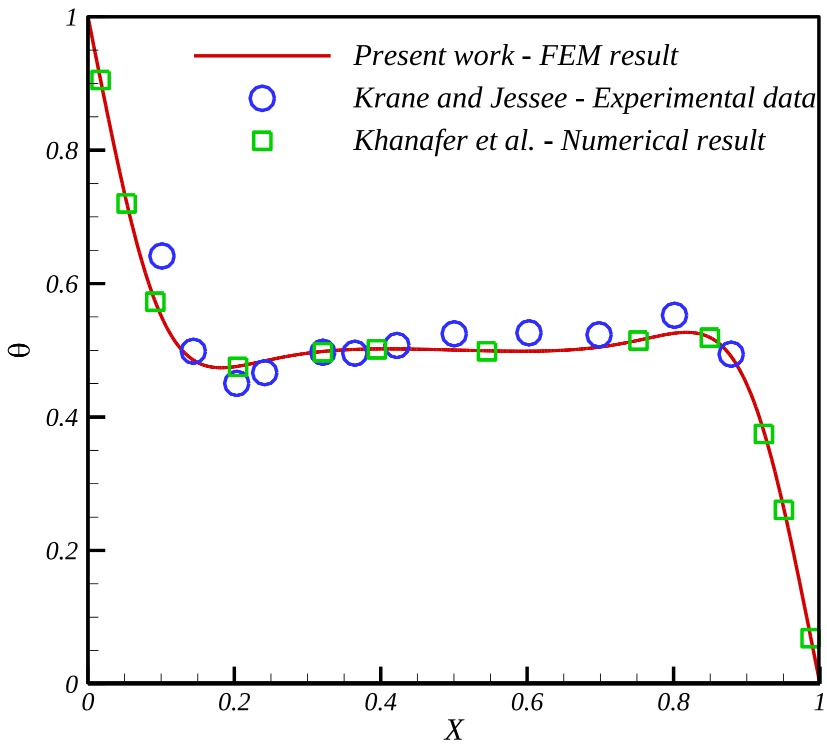

Fig. 2. Validation of current outcome with numerical result [25] and experimental data [26]

Table 1. Impact of ϕ on $Nu_{ave.}$ at disparate Ra and Ha

Ra	*Ha*	ϕ	$Nu_{ave.}$
10^4	0	0.01	1.3662
		0.03	1.4181
		0.05	1.4742
	40	0.01	1.2757
		0.03	1.3468
		0.05	1.4186
10^5	0	0.01	2.6305
		0.03	2.6445
		0.05	2.6742
	40	0.01	1.7803
		0.03	1.7836
		0.05	1.7922

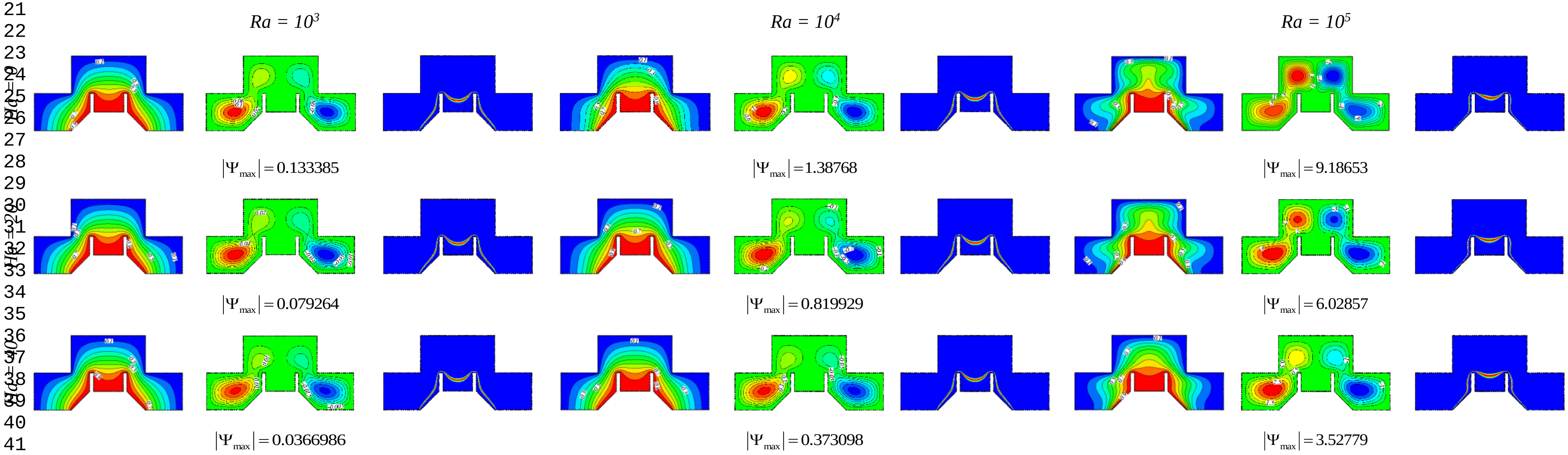

Fig. 3. Isotherms, streamlines, and heat capacity ratio for disparate values of Ra and Ha when AR=0.5, ϕ=0.05, Ste=0.313, Da=10^{-1} and θ_f=0.9

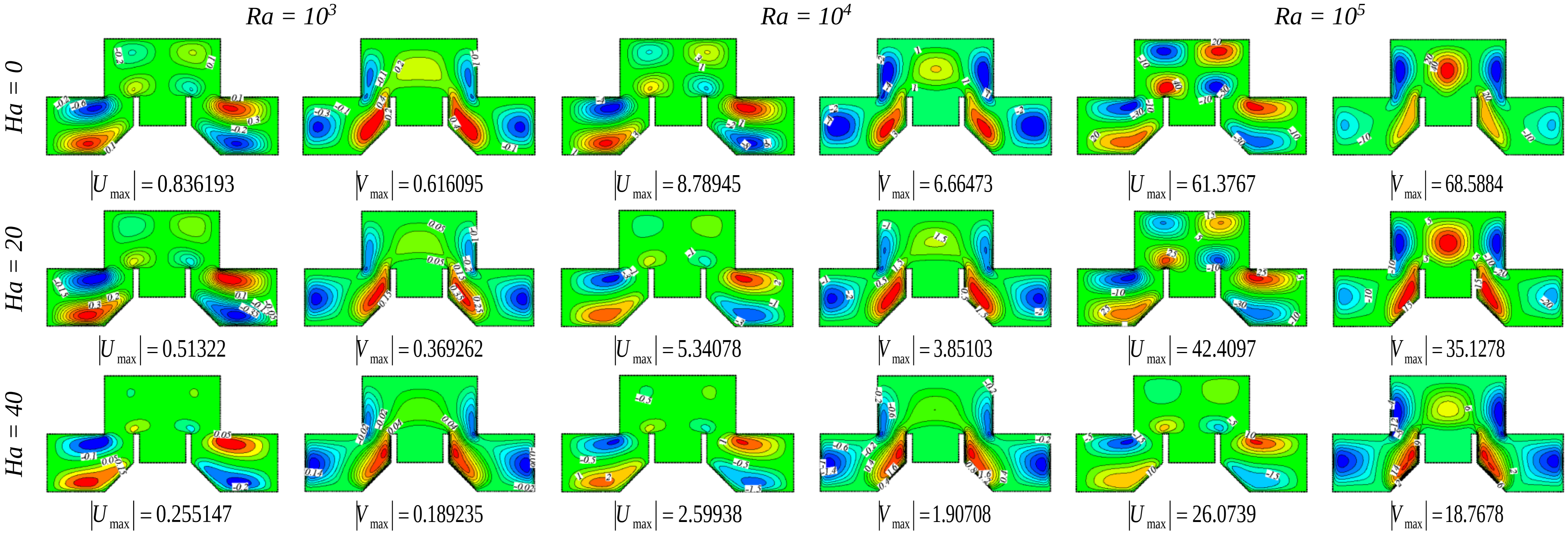

Fig. 4. Velocities (U,V) for disparate values of Ra and Ha when AR=0.5, ϕ=0.05, Ste=0.313, $Da=10^{-1}$ and θ_f=0.9

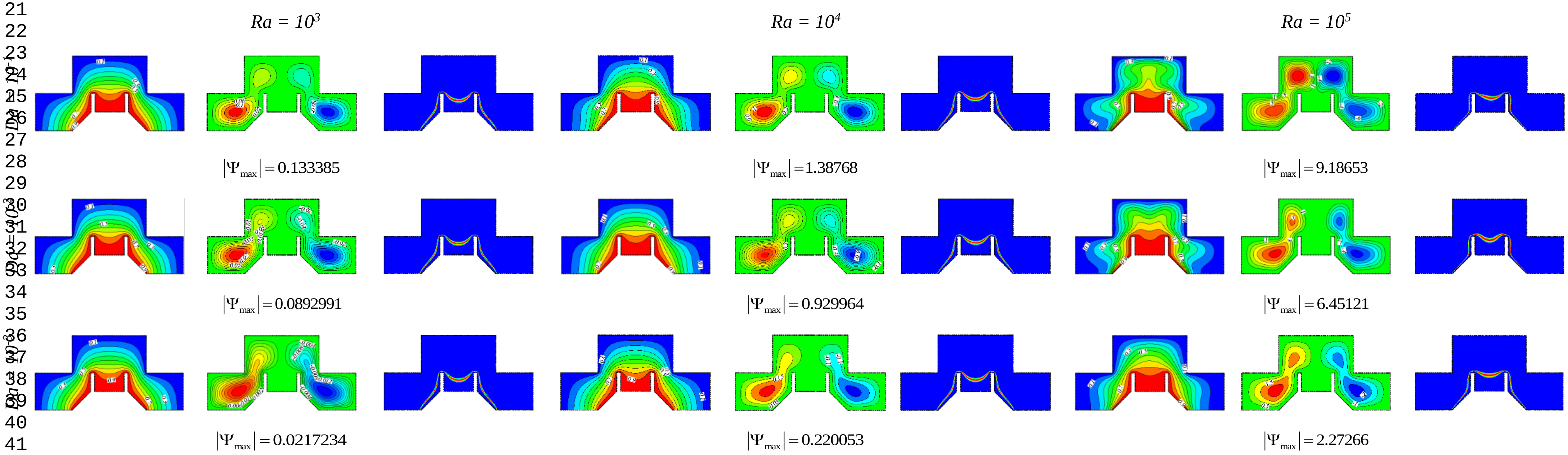

Fig. 5. Isotherms, streamlines, and heat capacity ratio for disparate values of Da at different Ra when AR=0.5, ϕ=0.05, Ste=0.313, Ha=0 and θ_f=0.9

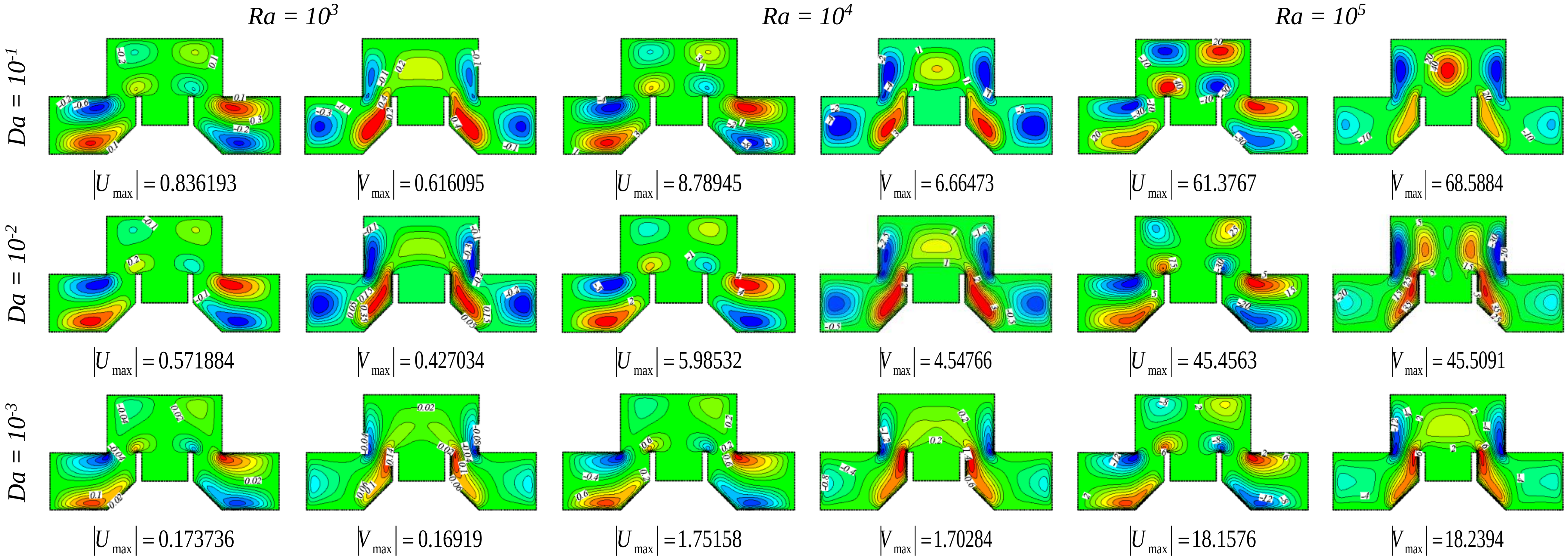

Fig. 6. Velocities (U,V) for disparate values of Da at different Ra when AR=0.5, ϕ=0.05, Ste=0.313, Ha=0 and θ_f=0.9

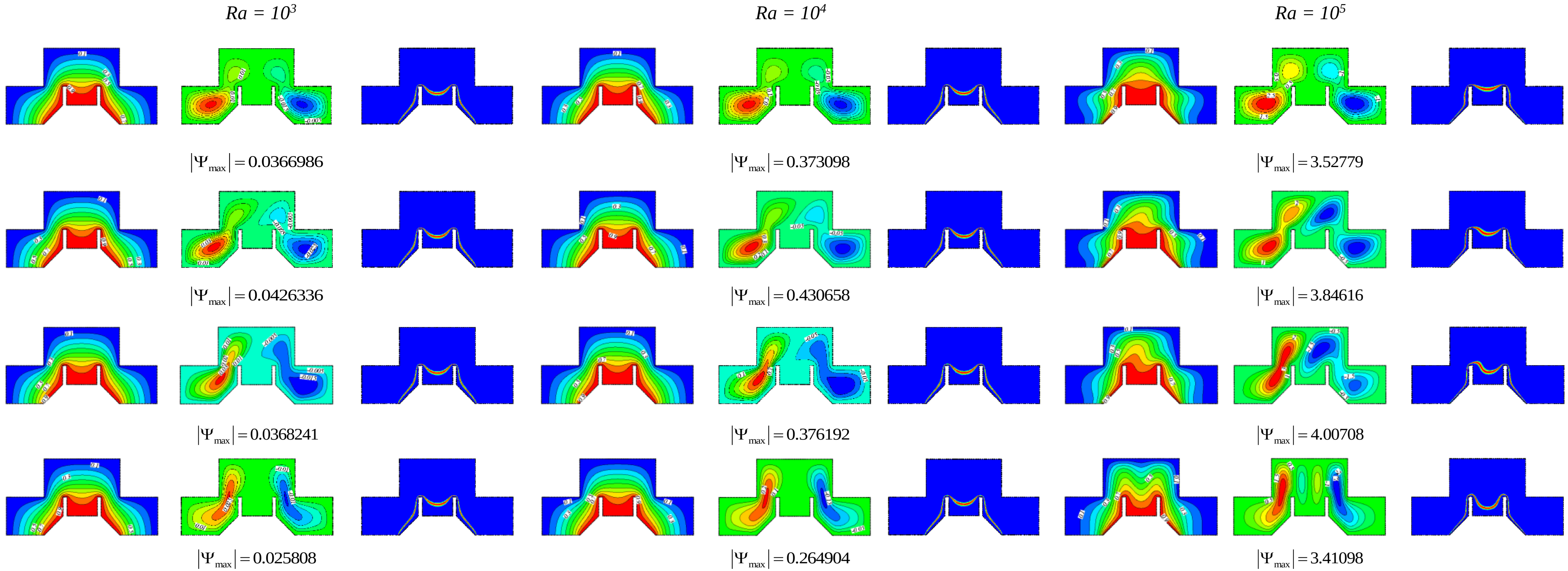

Fig. 7. Isotherms, streamlines, and heat capacity ratio for disparate values of γ at different *Ra* when AR=0.5, ϕ=0.05, Ste=0.313, Da=10^{-1}, Ha=40 and θ_f=0.9

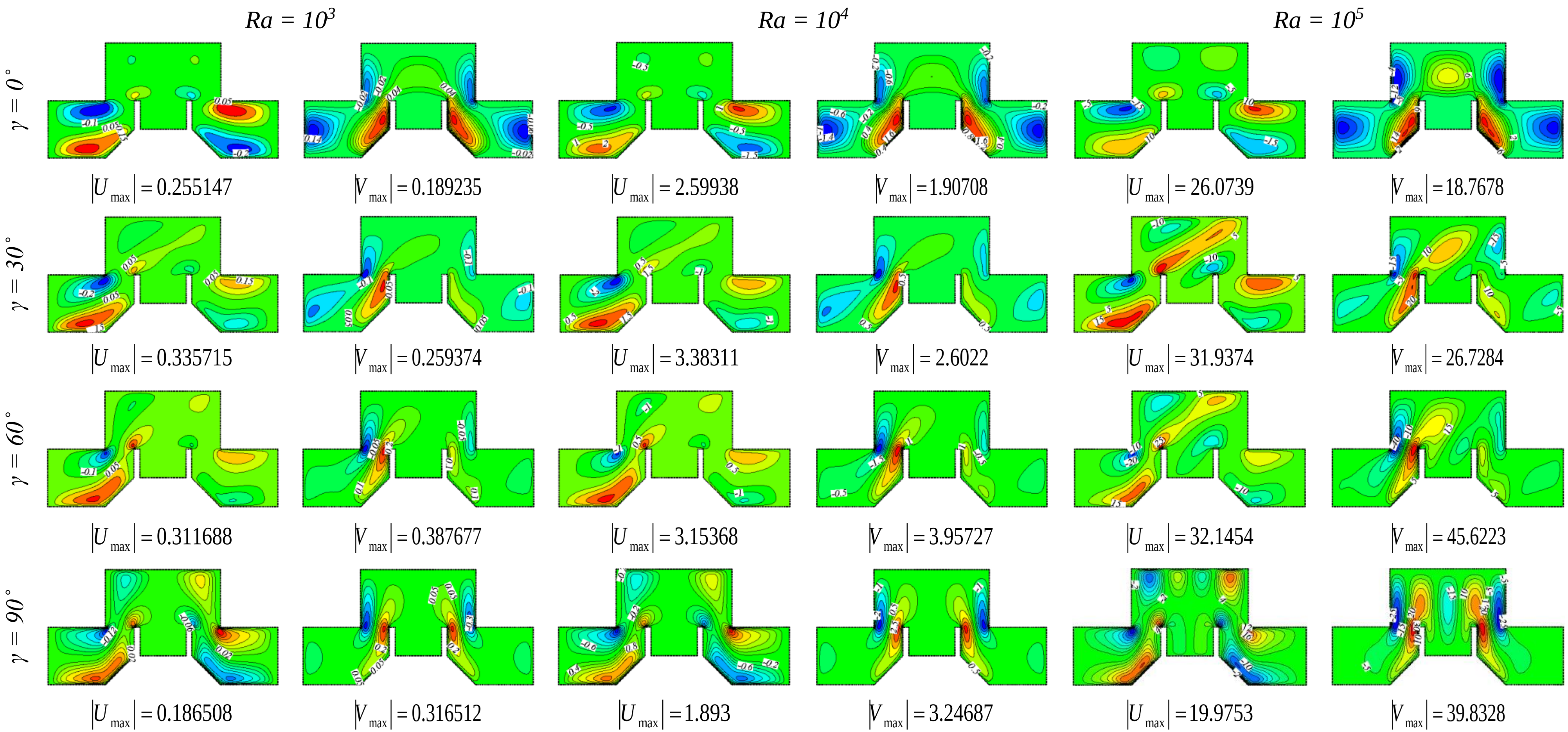

Fig. 8. Velocities (U,V) for disparate values of γ at different *Ra* when AR=0.5, ϕ=0.05, Ste=0.313, $Da=10^{-1}$, *Ha*=40 and θ_f=0.9

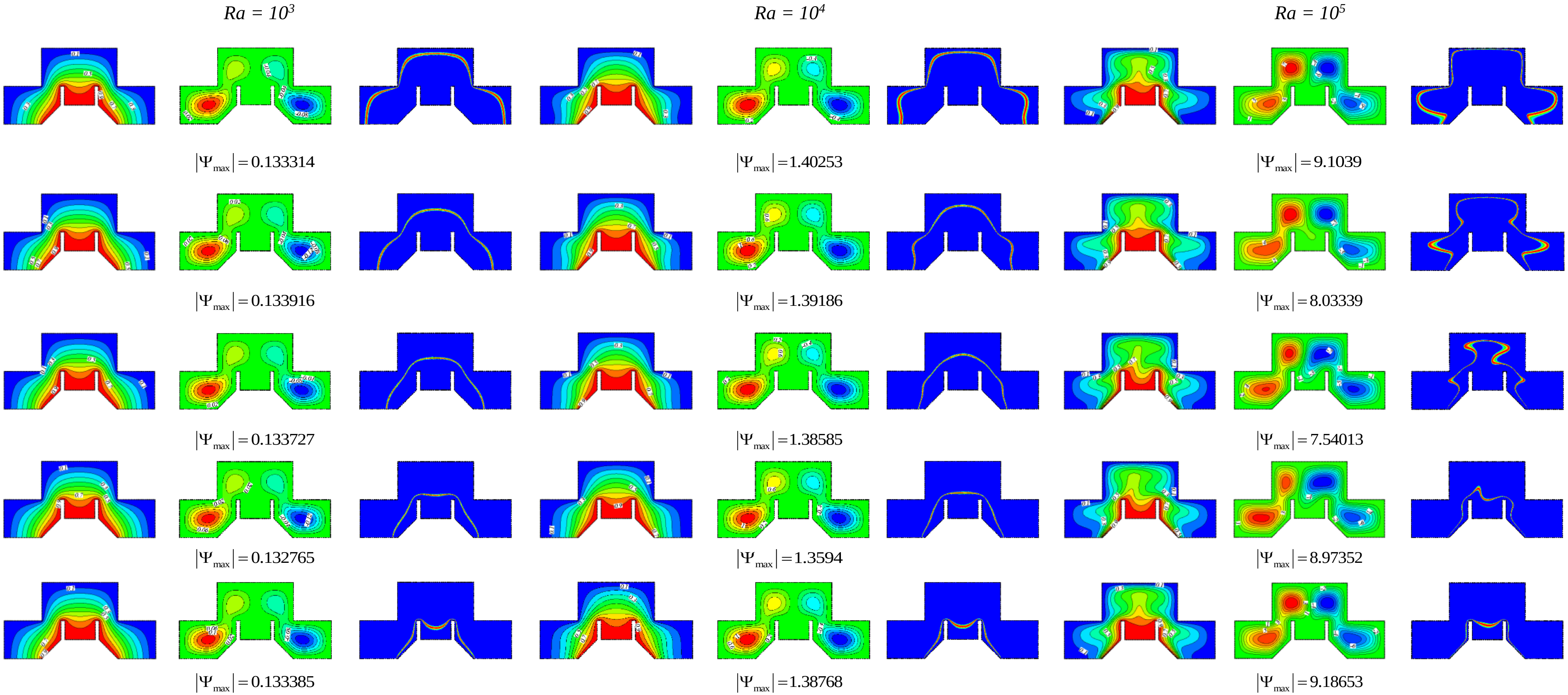

Fig. 9. Isotherms, streamlines, and heat capacity ratio for disparate values of θ_f at different Ra when AR=0.5, ϕ=0.05, Ste=0.313, Da=10^{-1} and Ha=0

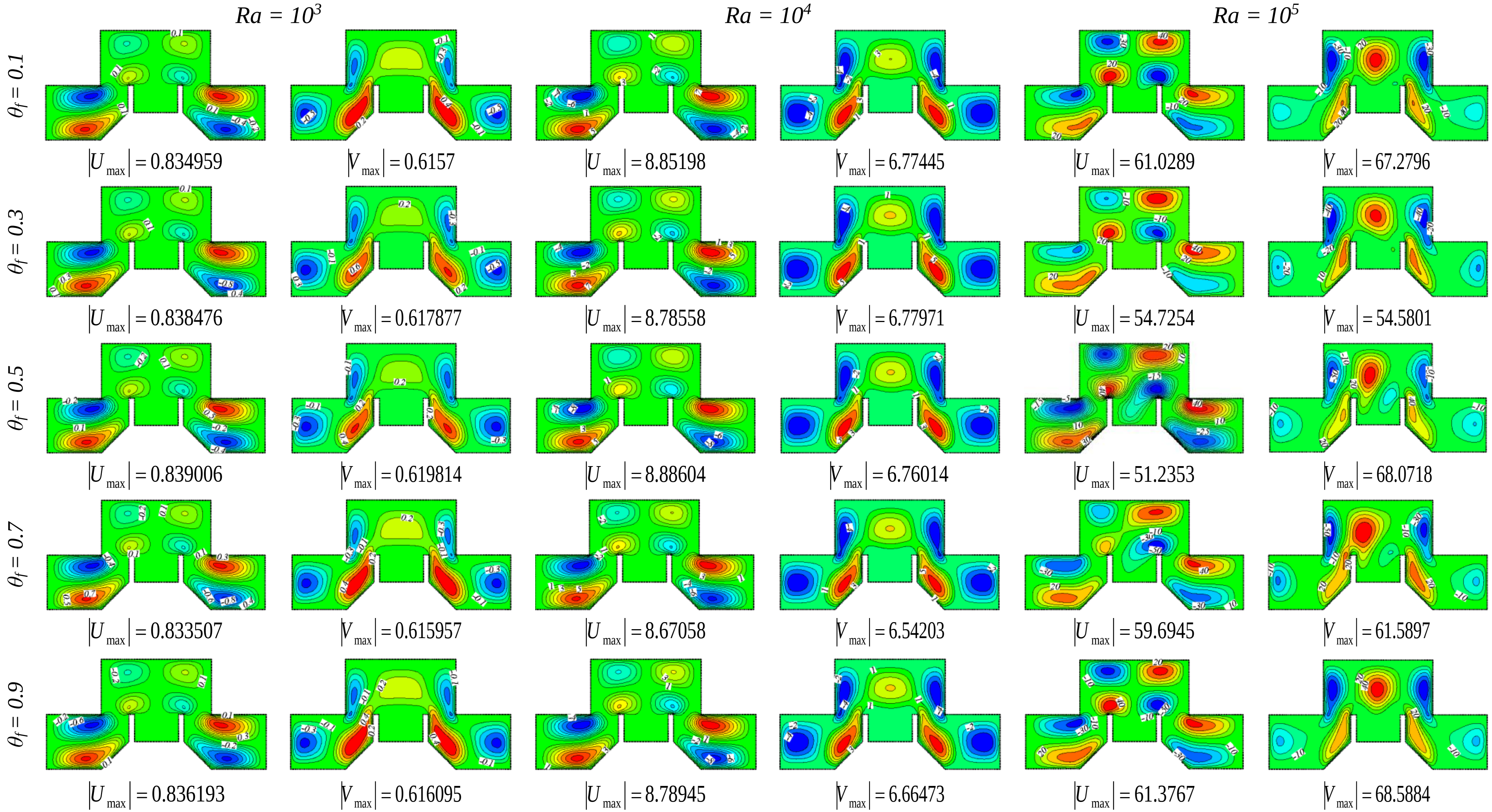

Fig. 10. Velocities (U,V) for disparate values of θ_f at different Ra when AR=0.5, ϕ=0.05, Ste=0.313, Da=10^{-1} and Ha=0

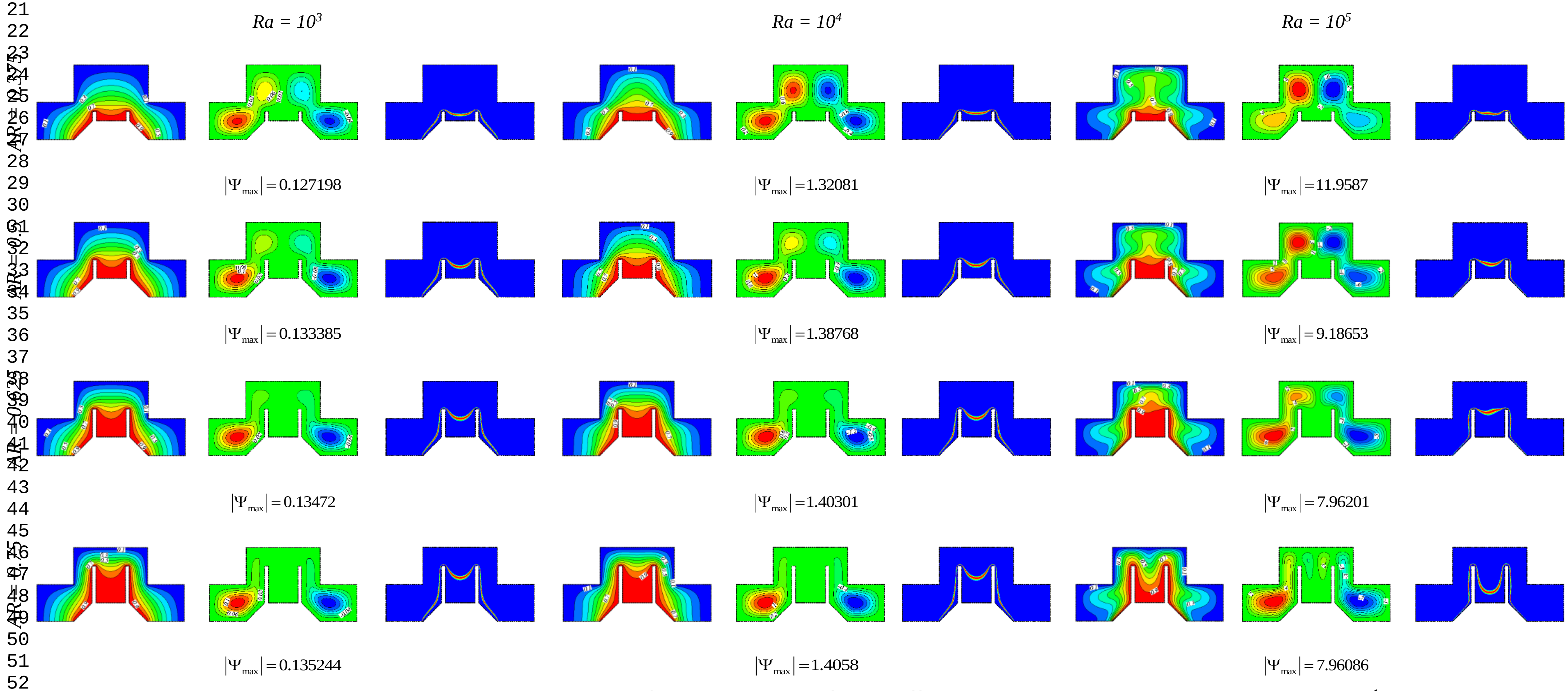

Fig. 11. Isotherms, streamlines, and heat capacity ratio for disparate values of *AR* at different *Ra* when ϕ=0.05, Ste=0.313, θ_f=0.9 and Da=10^{-1}

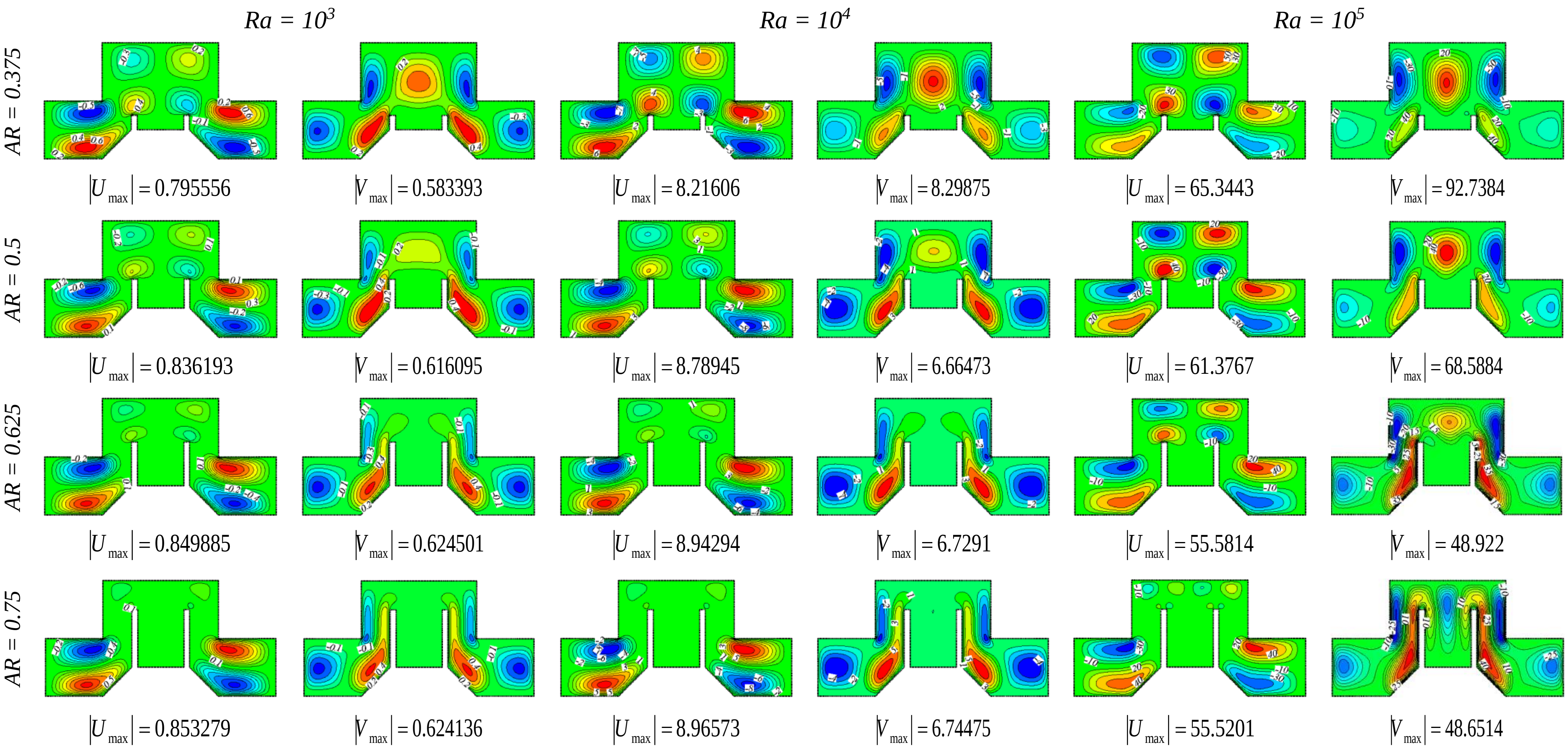

Fig. 12. Velocities (U,V) for disparate values of AR at different Ra when ϕ=0.05, Ste=0.313, θ_f=0.9 and Da=10^{-1}

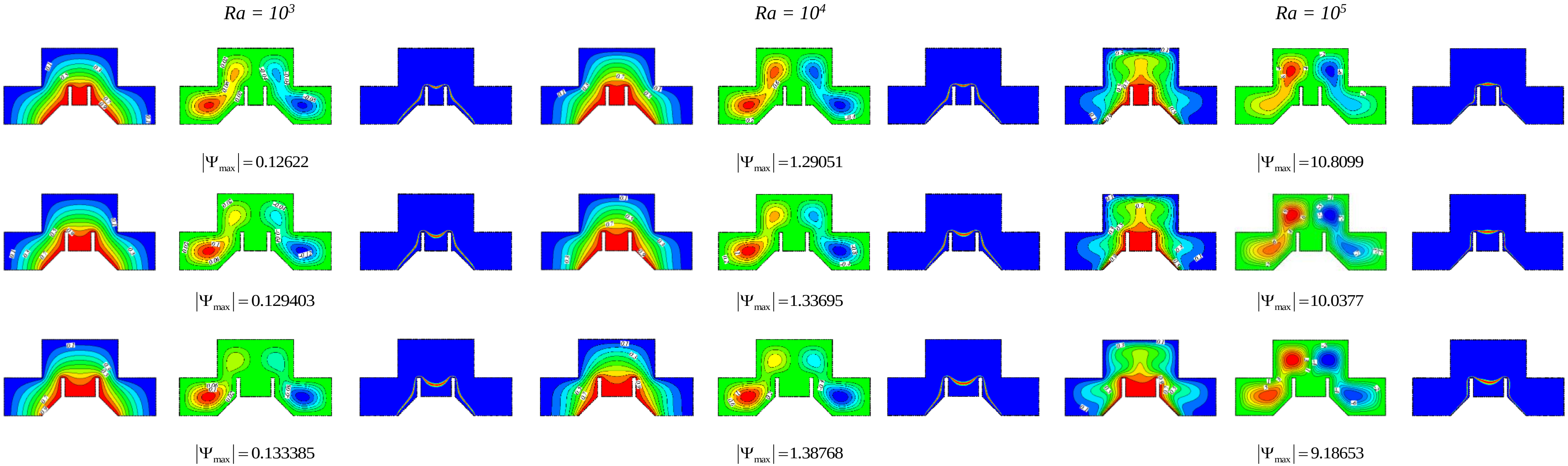

Fig. 13. Isotherms, streamlines, and heat capacity ratio for disparate values of δ at different Ra when AR=0.5, ϕ=0.05, Ste=0.313, Da=10^{-1} and θ_f = *0.9*

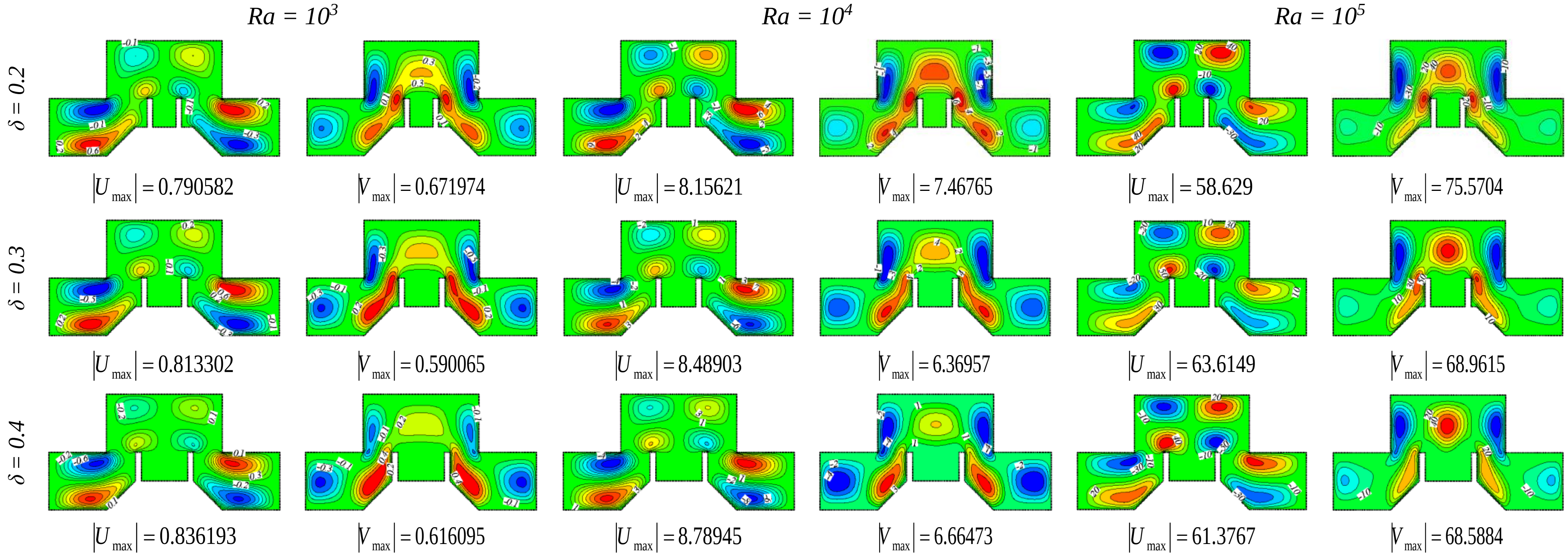

Fig. 14. Velocities (U,V) for disparate values of δ at different Ra when AR=0.5, ϕ=0.05, Ste=0.313, Da=10^{-1} and $\theta_f = 0.9$

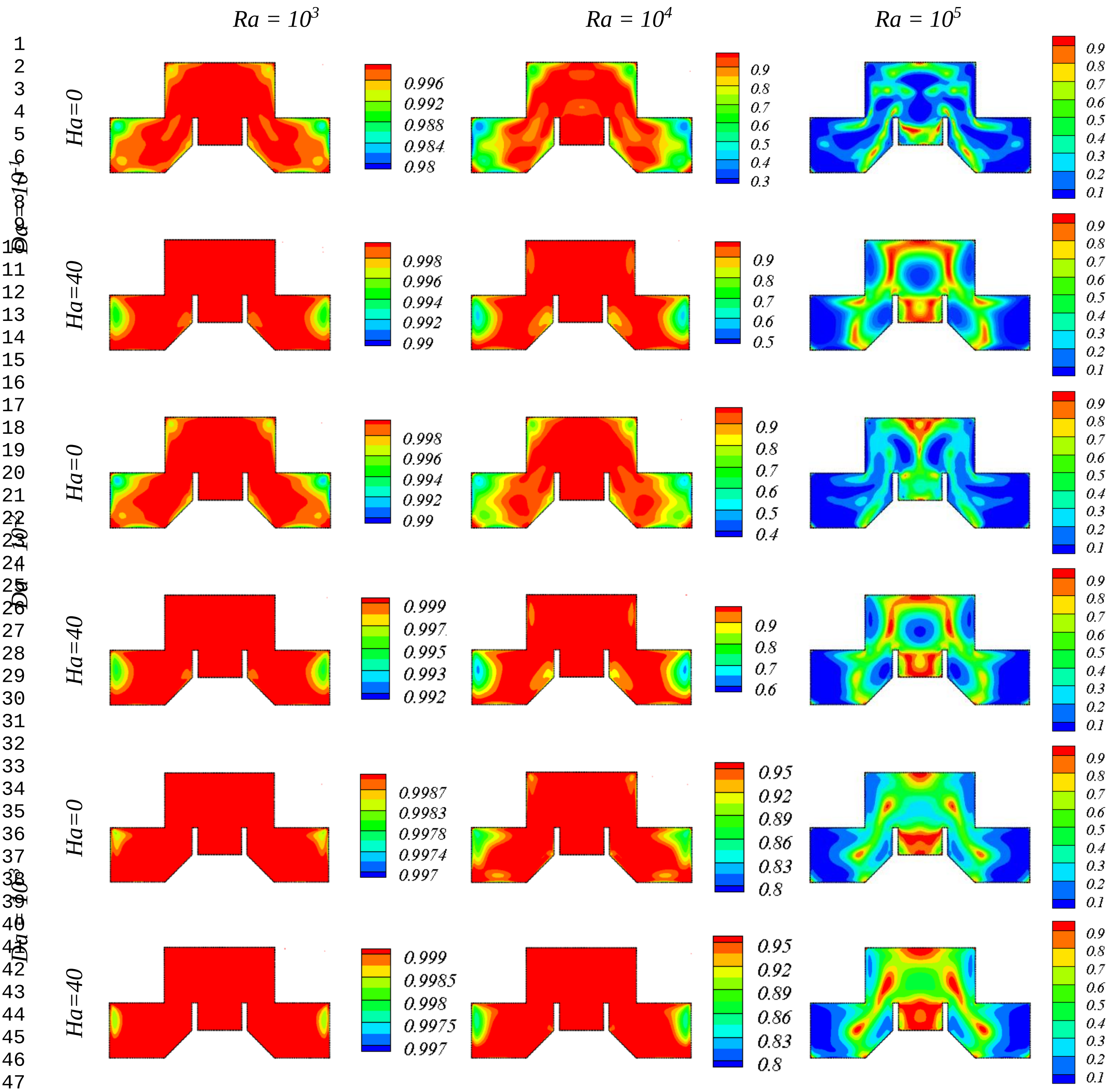

Fig. 15. Be_{loc} for for disparate values of AR, Ha, and Ra

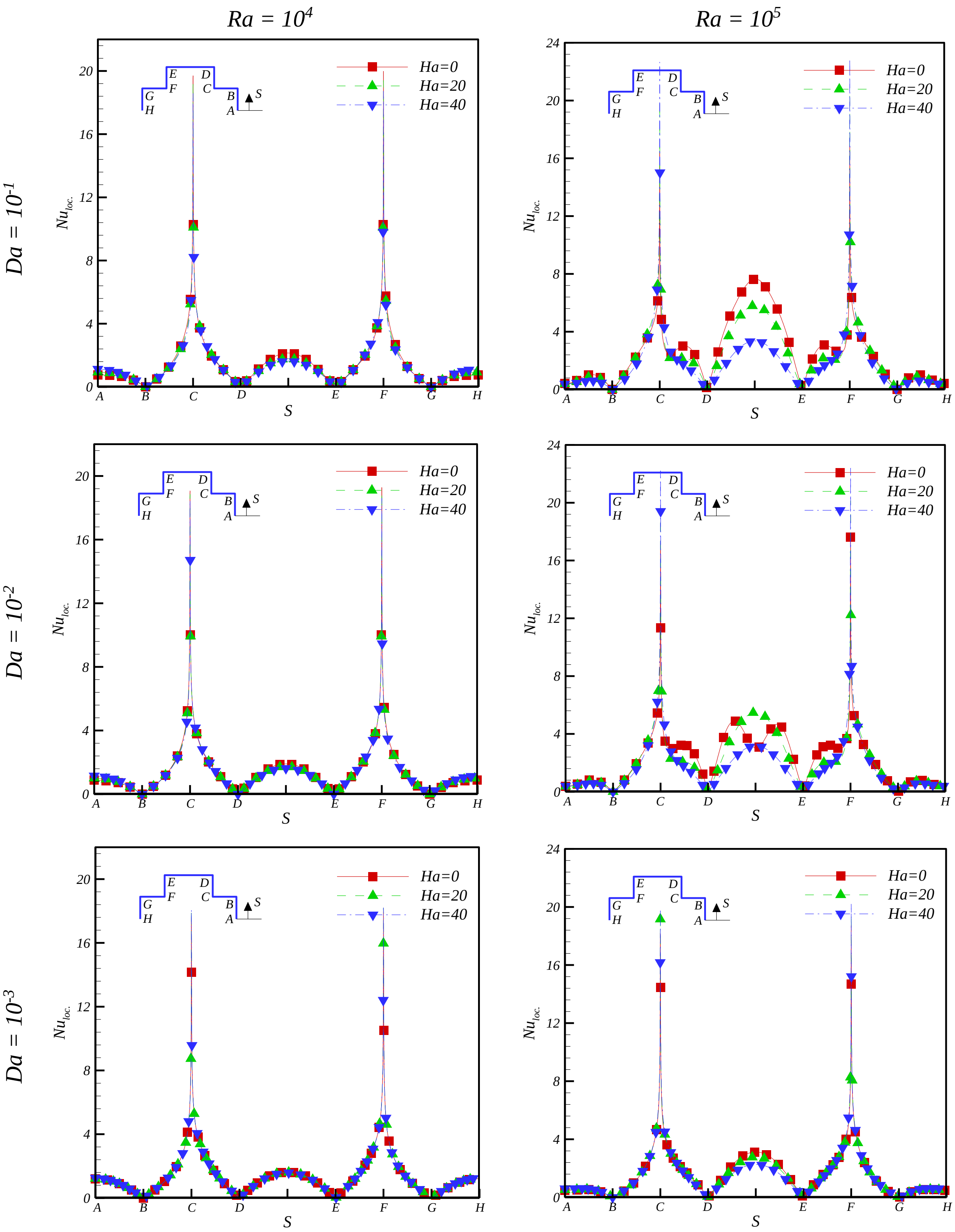

Fig. 16. Nu_{loc} for for disparate values of Da, Ha, and Ra

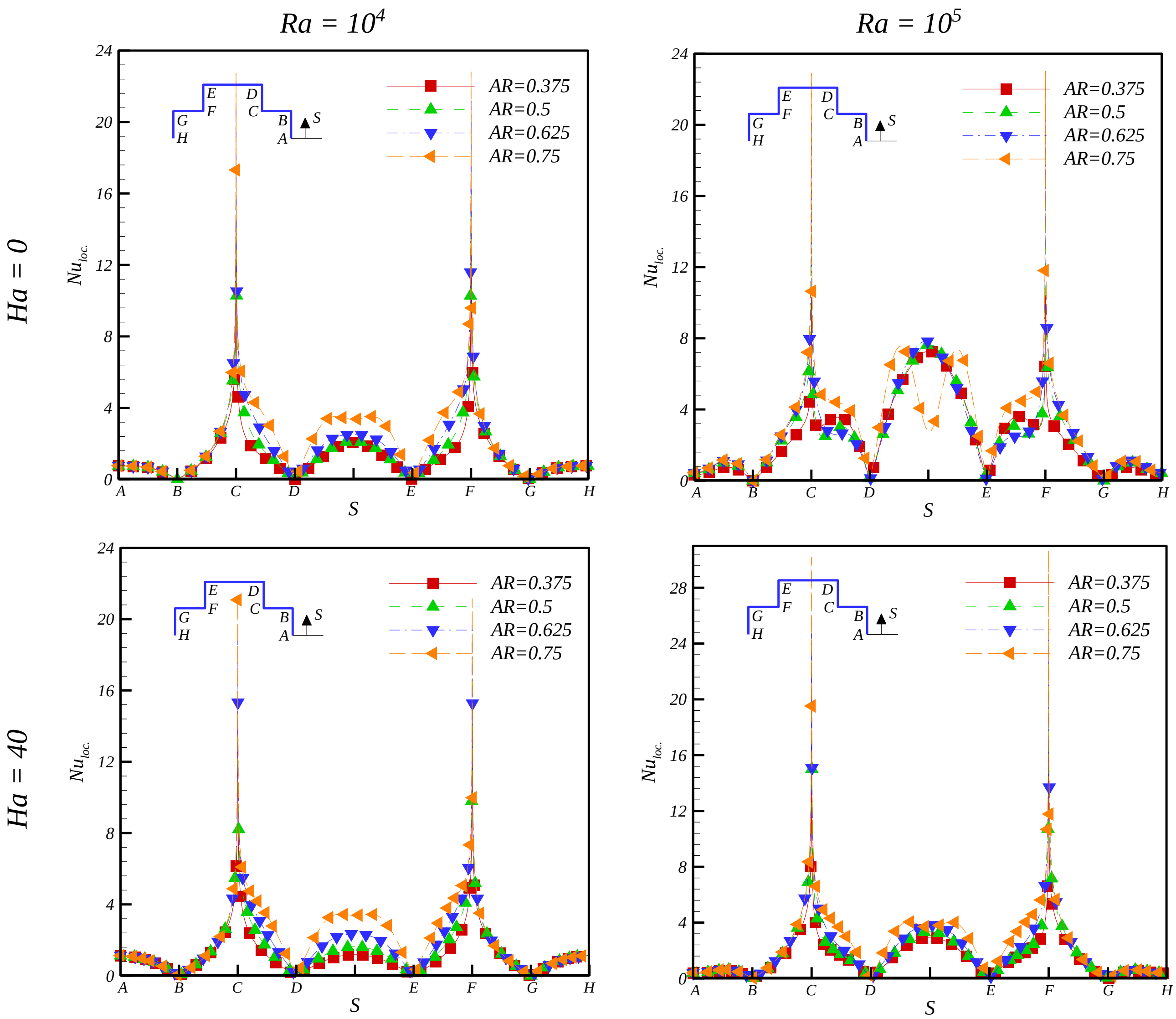

Fig. 17. Nu_{loc} for for disparate values of AR at different Ha and Ra

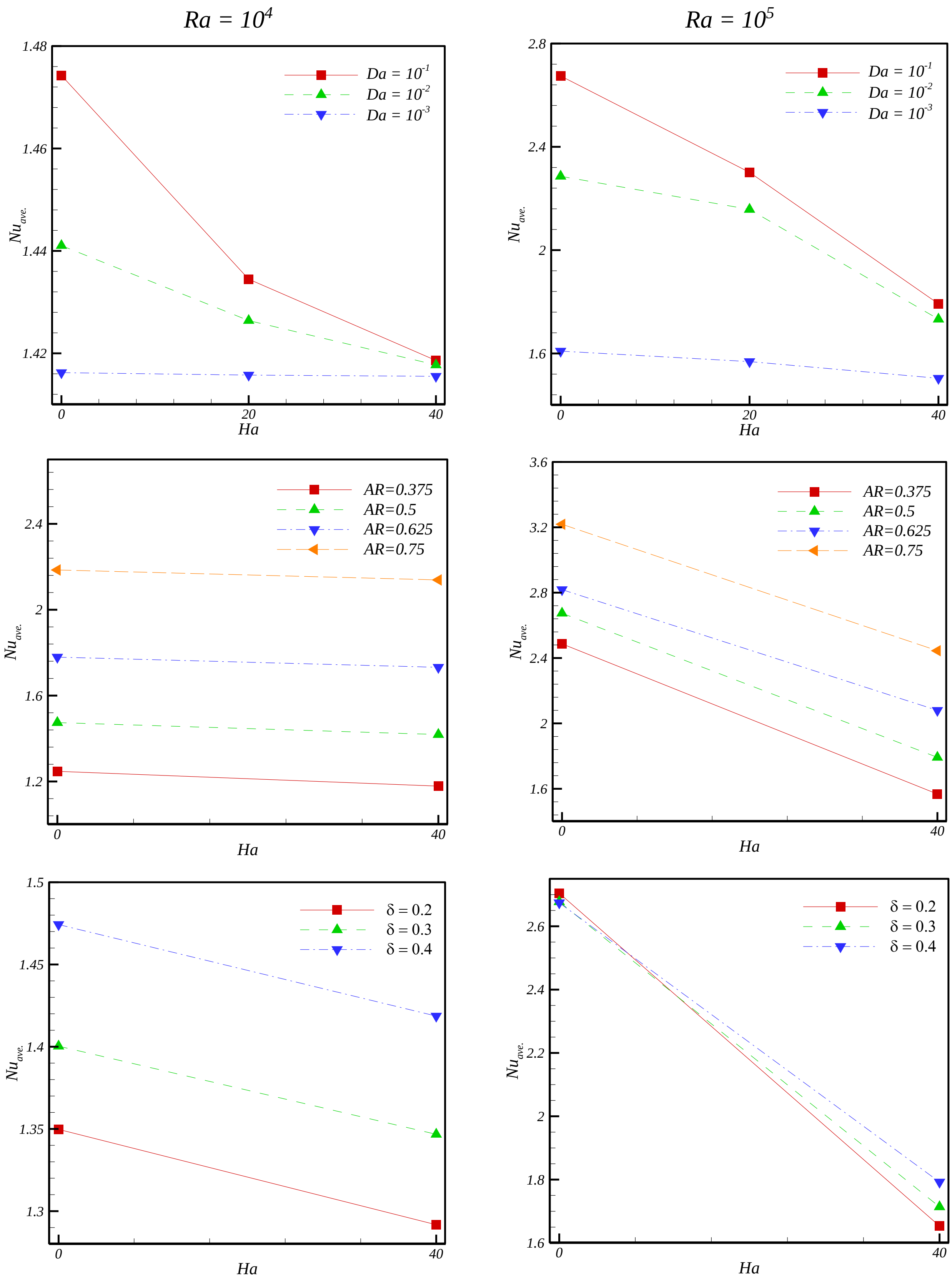

Fig. 18. $Nu_{ave.}$ for for disparate values of Da, Ha, Ra, AR ,and δ

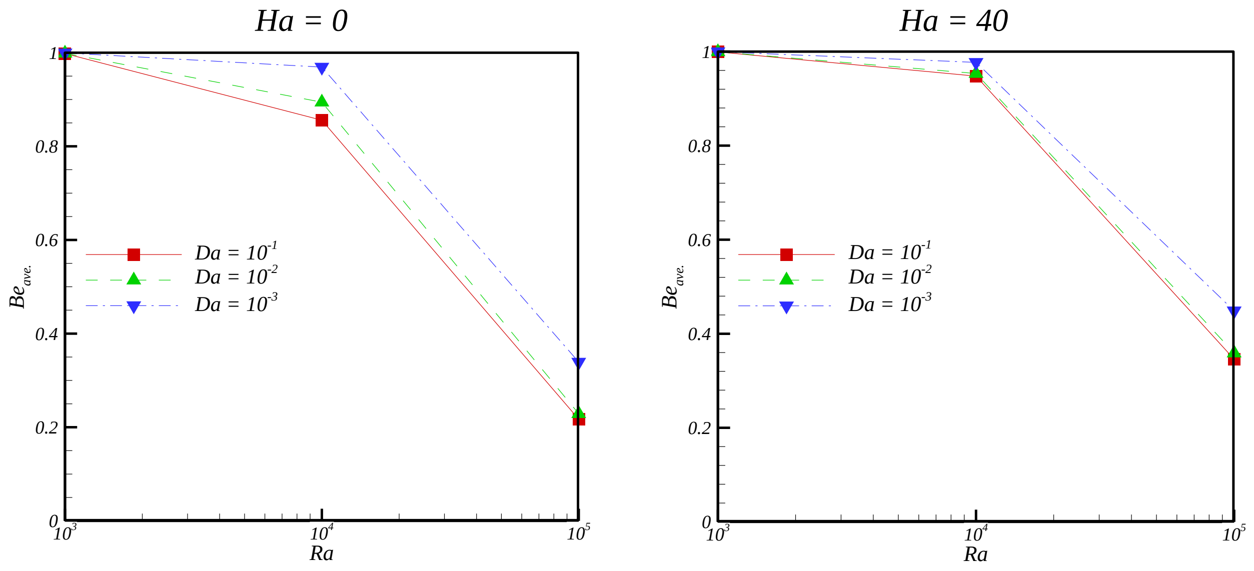

Fig. 19. $Be_{ave.}$ for for disparate values of Da, Ha, and Ra.

References

[1] Xu C, Yuan L, Xu Y, Hang W. Squeeze flow of interstitial Herschel–Bulkley fluid between two rigid spheres. Particuology 2010;8:360-64.

[2] Khan ZH, Rizwan-ul-Haq, Hussain ST, Hammouch Z. Flow and heat transfer analysis of water and ethylene glycol based Cu nanoparticles between two parallel disks with suction/injection effects. J. Mol. Liq. 2016;221:298-304.

[3] Khaled ARA, Vafai K. Hydromagnetic squeezed flow and heat transfer over a sensor surface. Int. J. Eng. Sci. 2004;42:509-19.

[4] Rashidi MM, Shahmohamadi H, Dinarvand S. Analytic approximate solutions for unsteady two-dimensional and axisymmetric squeezing flows between parallel plates. Math. Probl. Eng. 2008;2008:935095. doi:10.1155/2008/935095.

[5] Siddiqui AM, Irum S, Ansari AR. Unsteady squeezing flow of a viscous MHD fluid between parallel plates, a solution using the homotopy perturbation method. Math. Model. Anal. 2008;13:565-76.

[6] Ibrahim FN, Terbeche M. Solutions of the laminar boundary layer equations for a conducting power law non-Newtonian fluid in a transverse magnetic field. J. Phys. D: Appl. Phys. 1994;27:740-47.

[7] Watanabe T, Pop I. Thermal boundary layers in magnetohydrodynamic flow over a flat plate in the presence of a transverse magnetic field. Acta Mech. 1994;105:233-38.

[8] Khaled ARA, Vafai K. Heat transfer and hydromagnetic control of flow exit conditions inside oscillatory squeezed thin films. Numer. Heat Transfer. Part A 2003;43:239-58.

[9] Su W, Darkwa J, Kokogiannakis G. Review of solid–liquid phase change materials and their encapsulation technologies. Renew. Sustain. Energy Rev. 2015;48:373-91.

[10] Fang G, Li H, Yang F, Liu X, Wu S. Preparation and characterization of nanoencapsulated n-tetradecane as phase change material for thermal energy storage.

Chem. Eng. J. 2009;153:217-21.

[11] Qiu X, Li W, Song G, Chu X, Tang G. Fabrication and characterization of microencapsulated n-octadecane with different methylmethacrylate-based polymer shells, Sol. Energy Mater. Sol. Cells 2012;98:283-93.

[12] Jamekhorshid A, Sadrameli SM, Farid M. A review of microencapsulation methods of phase change materials (PCMs) as a thermal energy storage (TES) medium. Renew. Sustain. Energy Rev. 2014;31:531-42.

[13] Pielichowska K, Pielichowski K. Phase change materials for thermal energy storage, Prog. Mater Sci. 2014;65:67-123.

[14] Nematpour Keshteli A, Sheikholeslami M. Nanoparticle enhanced PCM applications for intensification of thermal performance in building: a review. J. Mol. Liq. 2019;274:516-33.

[15] Huang X, Alva G, Jia Y, Fang G. Morphological characterization and applications of phase change materials in thermal energy storage: a review. Renew. Sustain. Energy Rev. 2017;72:128-45.

[16] Moreno P, Solé C, Castell A, Cabeza LF. The use of phase change materials in domestic heat pump and air-conditioning systems for short term storage: a review. Renew. Sustain. Energy Rev. 2014;39:1-13.

[17] Hashim I, Alsabery AI, Sheremet MA, Chamkha AJ. Numerical investigation of natural convection of Al2O3-water nanofluid in a wavy cavity with conductive inner block using Buongiorno’s two-phase model. Adv. Powder Technol. 2019;30:399-414.

[18] Alsabery AI, Sheremet MA, Chamkha AJ, Hashim I. Impact of nonhomogeneous nanofluid model on transient mixed convection in a double lid-driven wavy cavity involving solid circular cylinder. Int. J. Mech. Sci. 2019;150:637-55.

[19] Sivaraj C, Sheremet MA. MHD natural convection and entropy generation of

ferrofluids in a cavity with a non-uniformly heated horizontal plate. Int. J. Mech. Sci. 2018;149:326-37.

[20] Ghalambaz M, Sheremet MA, Mehryan SAM, Kashkooli FM, Pop I. Local thermal non-equilibrium analysis of conjugate free convection within a porous enclosure occupied with Ag–MgO hybrid nanofluid. J. Therm. Anal. Calorim. 2019;135:1381-98.

[21] Tahmasebi A, Mahdavi M, Ghalambaz M. Local thermal nonequilibrium conjugate natural convection heat transfer of nanofluids in a cavity partially filled with porous media using Buongiorno's model, Numer. Heat Transf. Part A Appl. 2018;73:254-76.

[22] Ghalambaz M, Chamkha AJ., Wen D. Natural convective flow and heat transfer of Nano-Encapsulated Phase Change Materials (NEPCMs) in a cavity. Int. J. Heat Mass Transfer 2019;138:738-49

[23] Seyyedi SM, Dogonchi AS, Hashemi-Tilehnoee M, Waqas M, Ganji DD. Entropy Generation and Economic Analyses in a Nanofluid Filled L-Shaped Enclosure Subjected to an Oriented Magnetic Field. Appl. Therm. Eng. 2020;168:114789. doi: https://doi.org/10.1016/j.applthermaleng.2019.114789

[24] Usman M, Khan ZH, Liu MB. MHD natural convection and thermal control inside a cavity with obstacles under the radiation effects. Physica A 2019;535:122443.

[25] Khanafer K, Vafai K, Lightstone M. Buoyancy-driven heat transfer enhancement in a two-dimensional enclosure utilizing nanofluids. Int. J. Heat Mass Transfer 2003;46:3639-53.

[26] Krane RJ, Jessee J. Some detailed field measurements for a natural convection flow in a vertical square enclosure. Proceedings of the First ASME-JSME Thermal Engineering Joint Conference 1983;1:323-29.

Graphical Abstract:

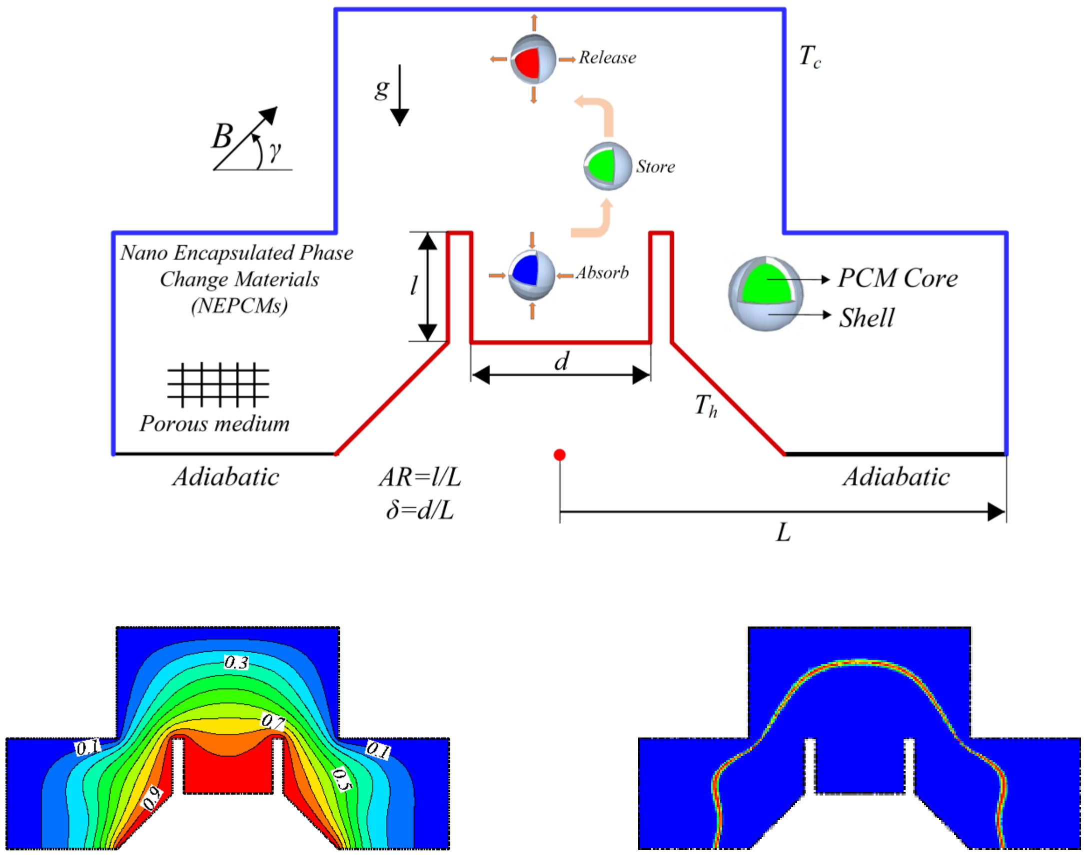

Declaration of interests

☒ The authors declare that they have no known competing financial interests or personal relationships that could have appeared to influence the work reported in this paper.

☐The authors declare the following financial interests/personal relationships which may be considered as potential competing interests: